



Chemoselective oxidative generation of *ortho*-quinone methides and tandem transformations

Muhammet Uyanik¹ , Kohei Nishioka, Ryutaro Kondo and Kazuaki Ishihara¹

***ortho*-Quinone methides are useful transient synthetic intermediates in organic synthesis. These species are most often generated in situ by the acid- or base-mediated transformation of phenols that have been pre-functionalized at a benzylic position, or by biomimetic oxidation of the corresponding *ortho*-alkylphenols with metal oxidants or transition-metal complexes. Here we describe a method for the transition-metal-free oxidative generation of *o*-QMs from *ortho*-alkylarenols, using hypoiodite catalysis under nearly neutral conditions, which can then be applied in one-pot tandem reactions. This method for the chemoselective oxidative generation of *ortho*-quinone methides may prove superior to previous methods with respect to environmental issues and scope, and can be applied to various tandem reactions such as inter- or intramolecular [4 + 2] cycloaddition, oxa-6 π -electrocyclization, conjugate addition and spiroepoxidation.**

ortho-Quinone methides (*o*-QMs) are extensively used as highly reactive transient intermediates in organic synthesis and biological processes^{1–5}. Because of the combination of neutral non-aromatic and zwitterionic aromatic resonance structures, *o*-QMs have a distinctive chemical reactivity that enables them to act as key intermediates in several biological processes such as lignification in plants, the formation of epidermis and melanin in animals, alkylation of DNA and proteins, crosslinking of DNA, and so on^{1,2,6}. Additionally, several natural products and clinical drugs exhibit their antitumour or antibacterial activities via *o*-QM species upon bio-reductive or bio-oxidative activation in vivo^{1,2,7}.

Since the 2000s, *o*-QMs have been widely used as versatile intermediates in organic synthesis^{1–5}. *o*-QMs react with various classes of reagents by three typical reaction pathways: 1,4-addition of nucleophiles, [4 + 2] cycloaddition with dienophiles and oxa-6 π -electrocyclization. Because most *o*-QMs are unstable and, therefore, mostly nonisolable, the scope of these reactions generally depends on the reaction conditions used for the generation of the *o*-QMs in situ. Conventionally, these unstable intermediates are generated in situ by thermolysis, photolysis, tautomerization or, especially, acid- or base-promoted transformations¹. However, an appropriate leaving group (LG) at the *ortho*-benzylic position of phenols is generally required (Fig. 1a, left)^{1,2}. Biomimetic oxidative generation from the corresponding *ortho*-alkylphenols has also been developed¹. However, generally, toxic heavy-metal oxidants have been required (Fig. 1a, right)^{1,8–12}. Recently, transition-metal-catalysed oxidative generation of *o*-QMs under aerobic conditions has also been reported^{13,14}. However, the substrate scope with respect to the *o*-QM precursor was limited to highly reactive sesamol derivatives¹³ or 3-alkyl-2-naphthols even under harsh reaction conditions¹⁴. Although *o*-QMs are generated chemoselectively in vivo by oxidase^{2,7}, chemoselective oxidation is generally difficult in synthetic organic chemistry¹.

Based on serendipitous findings, we report here the first transition-metal-free oxidative generation of *o*-QMs from *ortho*-alkylarenols using hypoiodite catalysis^{15–18} and the synthetic application of *o*-QMs as reactive intermediates to tandem reactions (Fig. 1b). The hypoiodite salts are generated in situ from the corresponding quaternary ammonium iodides in the presence of mild, safe and

inexpensive oxidants such as hydrogen peroxide or alkyl peroxides. This method for the chemoselective generation of *o*-QMs is superior to previous methods with respect to not only environmental issues but also the substrate scope, especially with respect to coupling partners, and can be comprehensively applied to various oxidative tandem reactions such as [4 + 2] cycloaddition (including self-dimerization and -trimerization), oxa-6 π -electrocyclization, conjugate addition and spiroepoxidation (a new reaction).

Results and discussion

Recently, we reported the hypoiodite-catalysed peroxidative dearomatization of phenols with *tert*-butyl hydroperoxide (TBHP) as an oxidant and coupling reagent¹⁹. When 1,3-dimethyl-2-naphthol **1a** was used as a substrate, the unexpected spiro-dimer chroman **4a** was obtained in 30% yield along with the desired peroxide **2** and undesired 1,2-quinol **3** (Fig. 2a). *o*-QM intermediate **5** was assumed to be generated in situ and then to undergo immediate self-condensation to the corresponding spiro-dimer **4a**. We speculated that, while peroxide **2** and quinol **3** might be obtained via ‘path a’, which involves a nucleophilic addition of ammonium *tert*-butyl hydroperoxide or hydroxide to the *ortho*-position of aryl hypoiodite intermediate **1-I**, *o*-QM **5** might be generated via ‘path b’, which involves β -elimination of a benzylic proton. The enhanced acidity of benzylic protons in **1-I** might lead to competition with *ipso*-addition and deprotonation events. In fact, we observed several unidentified by-products for the oxidative dearomatization of some phenols using hypoiodite catalysis. Because *o*-QMs are highly reactive compounds that might react unselectively with various reagents or solvents present in the reaction medium to give a complex mixture of various types of products (sometimes oligomeric compounds), we could not determine these side products in most cases. Thanks to the relatively clean reaction in this particular case, we serendipitously found a new application of hypoiodite catalysis, that is, the oxidative generation of *o*-QMs.

To develop a chemoselective generation of *o*-QMs, we investigated the reaction parameters using **1a** as a model substrate (see Supplementary Table 1 for details). To suppress ‘path a’, we reduced the amount of oxidant used to 1.1 equiv. under otherwise identical conditions in the presence of tetrabutylammonium iodide

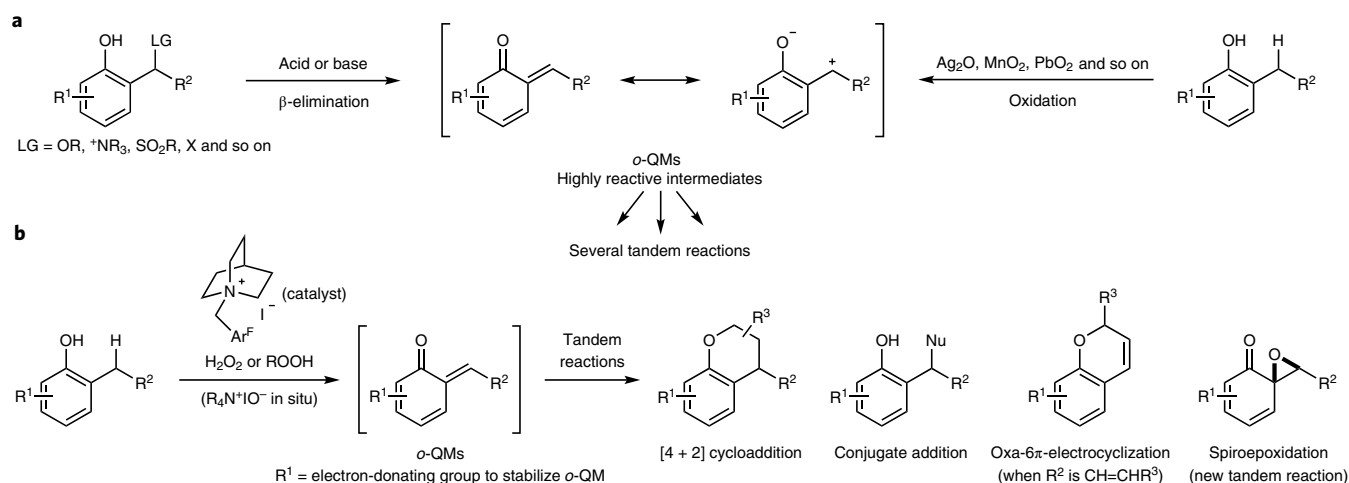


Fig. 1 | Generation of *o*-QMs and synthetic application. **a**, Conventional methods for the in situ generation of *o*-QMs including acid- or base-promoted transformations or oxidation of the corresponding *ortho*-alkylphenols, which often requires an appropriate LG or toxic heavy-metal oxidants, respectively. **b**, Chemoselective oxidative generation of *o*-QMs catalysed by quaternary ammonium hypoiodite under mild conditions and the application of the *o*-QMs to various tandem reactions (this work). R^3 , alkyl or aryl groups.

(10 mol%) in dichloroethane (DCE), and the yield of **4a** was significantly improved. The use of a 30% aqueous solution of hydrogen peroxide as an oxidant shortened the reaction time at room temperature with higher chemoselectivity. Moreover, a brief screening of solvents revealed that a faster reaction in acetonitrile gave **4a** quantitatively (Fig. 2b). To improve the reaction rate further, we focused on the quaternary cations of the catalyst (Fig. 2c). More than 26 h were required for the reaction to complete using tetrabutylammonium or tetramethylammonium iodide as a commercially available catalyst under optimized conditions. We examined various ammonium iodides **6a–d** derived from structurally compact quinuclidine. Although the reaction rate was only slightly improved with the use of **6a–c**, the use of catalyst **6d** bearing electron-withdrawing groups enhanced the reaction rate significantly, and **4a** was obtained quantitatively after 12 h. To ascertain the structural and electronic influence of the ammonium cation, catalyst **6e**, which is not quinuclidine-derived but bears electron-withdrawing groups, was examined and found to exhibit reactivity similar to those of **6a–c**. These results indicate that both the structurally compact and electronically deficient features of catalyst **6d** might be crucial to induce high reactivity. Metal cations were also investigated, and inexpensive sodium iodide was found to exhibit a reactivity similar to that of ammonium iodide **6d** in acetonitrile (see Supplementary Tables 2 and 3 for details). However, in sharp contrast with the ammonium iodides, the catalytic activity of sodium iodide decreased remarkably in common organic solvents (except acetonitrile) or when alkyl hydroperoxides were used as an oxidant instead of hydrogen peroxide.

In comparison, *o*-QMs derived from phenols are prone to trimerization through two sequential $[4 + 2]$ cycloaddition reactions¹. However, oxidation of 4-methoxyphenol **7a** under conditions identical to those for 2-naphthol **1a** gave trimer **8a** in 54% yield along with 1,4-quinone in 25% yield and several unidentified by-products (Fig. 2d; see Supplementary Table 3 for details). Consistent with previous reports^{9,10}, a single diastereomer of **8a** could be isolated, and its structure was confirmed by single-crystal X-ray diffraction analysis. To suppress undesired oxidation pathways, we investigated alkyl hydroperoxides as weaker oxidants²⁰. Although the use of TBHP gave a complex mixture of **8a**, 1,4-quinone and a peroxy adduct in a combined yield of 20%, a chemoselective reaction could be achieved by using an anhydrous solution of cumene hydroperoxide (CHP) to give the desired product **8a** in 60% yield. Moreover, the reaction rate

was increased in dichloroethane, and **8a** was obtained in 89% isolated yield (Fig. 2d). Similarly, (\pm)-schefflone (**8b**)^{9,10}, a structurally complex pentacyclic natural product, was obtained from the oxidation of espintanol (**7b**) under mild conditions in 72% yield (Fig. 2d).

The application of *o*-QMs to intermolecular coupling reactions with external nucleophiles is often difficult because of the high tendency towards self-dimerization, and is limited to relatively stable *o*-QMs (refs. 1,21,22). We succeeded in extending our catalytic oxidative generation method to the chemoselective $[4 + 2]$ cycloaddition of *o*-QMs with various external dienophiles. By using highly active catalyst **6d** under optimized conditions for both naphthols and phenols, we obtained the corresponding chromans **10aa** and **11aa**, respectively, in high yields, through $[4 + 2]$ cycloaddition of *o*-QMs generated in situ from **1a** or **7a** with ethyl vinyl ether (**9a**) as an electron-rich dienophile (Fig. 2e). Notably, the use of an excess amount of dienophile was crucial to prevent dimerization or trimerization reactions. By sharp contrast, the self-dimerization or trimerization of **1a** or **7a** competed with $[4 + 2]$ cycloaddition even in the presence of an excess amount of **9a** with the use of stoichiometric amounts of Ag_2O or MnO_2 (Fig. 2e).

Various naphthols **1** (method A) and phenols **7** (method B) were examined for oxidative $[4 + 2]$ cycloaddition under the optimized conditions (Table 1). A variety of dienophiles such as ethyl vinyl ether (**9a**), 2-methoxypropene (**9b**), silyl enol ether (**9c**), ethyl propenyl ether (**9d**), vinyl thioethers (**9e** and **9f**), vinyl amide (**9g**) and *N*-methylindole (**9h**) could be successfully used as coupling partners. The corresponding chromans **10** and **11** were obtained in high to excellent yields. Several functional groups such as bromo, allyl, alkenyl, cyclopropyl, alkoxy, acetal, thioacetal and amination groups were tolerated under these mild conditions. However, imines²³ could not be used as a dienophile due to preferential undesired oxidation of these species under our conditions. Notably, the oxidative cycloaddition of **1a** or **7c** with indole **9h** gave chroman **10ah** or **11ch** initially, which were transformed to the corresponding 1,4-adducts **12a** or **12b** during purification by SiO_2 column chromatography or in situ, respectively. Interestingly, the use of a 2:1 *Z/E* mixture of **9d** as a dienophile gave the corresponding **10ad** with a moderate *trans* selectivity (d.r. 2.5:1), which was confirmed by a nuclear Overhauser effect (nOe) analysis. Additionally, the oxidative coupling of 1-naphthols **1h–j** bearing secondary alkyl groups at the benzylic positions afforded the corresponding *endo*-cycloadducts **10** exclusively, presumably via the corresponding *E*-configured *o*-QMs (refs. 1,24).

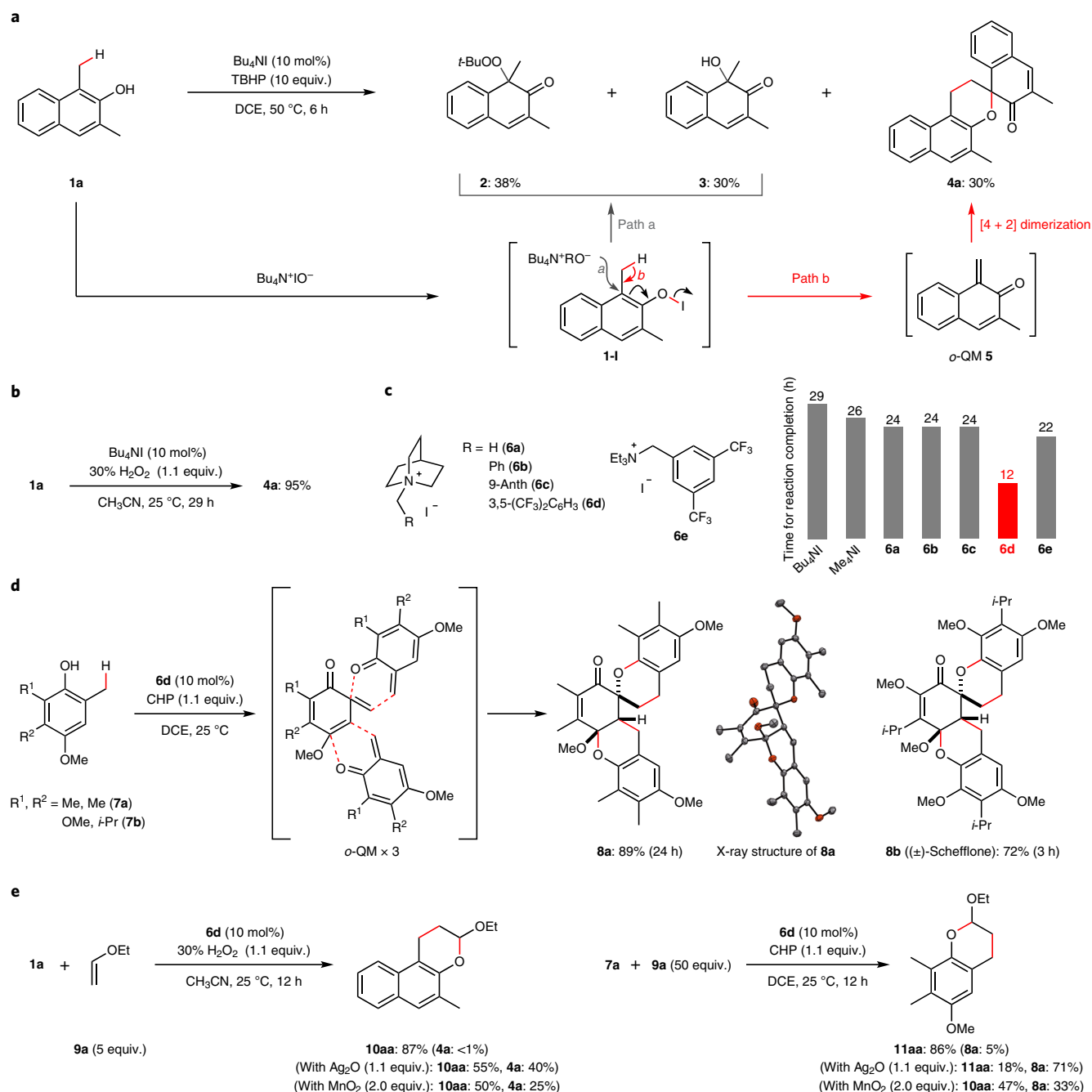
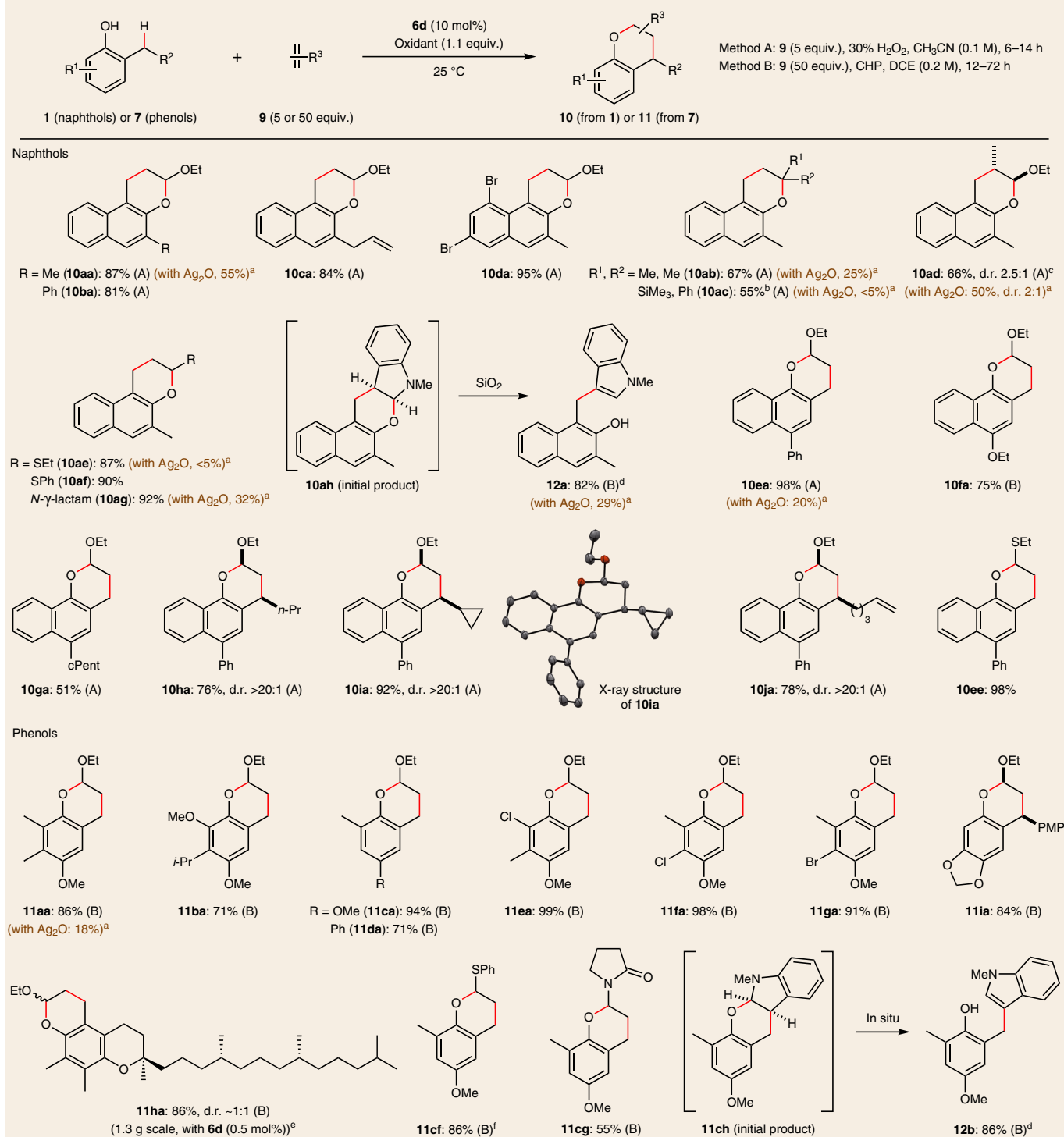


Fig. 2 | Oxidative generation of *o*-QMs catalysed by ammonium hypoiodite. **a**, Serendipitous finding of the oxidative generation of *o*-QMs catalysed by quaternary ammonium hypoiodite. While dearomative addition of ammonium *tert*-butyl hydroperoxide or hydroxide to the *ortho*-position of aryl hypoiodite intermediate **1-I** might afford the corresponding peroxide **2** and quinol **3** (path a), respectively, β -elimination of a benzylic proton might afford the *o*-QM **5** (path b), which would then self-dimerize to spirochroman **4a**. **b**, Oxidative dimerization of 2-naphthol **1a** to **4a** under optimized conditions (see Supplementary Table 1 for details). **c**, Evolution of quaternary ammonium cation to induce high reactivity (see Supplementary Table 2 for details). The time required to complete the reaction of **1a** to **4a** (>95%) is shown. Both structurally compact and electronically deficient features of catalyst **6d** might be crucial to induce high reactivity. **d**, Oxidative trimerization of phenols **7a** and **7b** and synthesis of (\pm)-schefflone (**8b**), a pentacyclic natural product. The structure of **8a** was confirmed by single-crystal X-ray diffraction analysis. Hydrogen atoms are omitted for clarity. Grey, carbon; red, oxygen. **e**, Chemoselective oxidative [4 + 2] cycloaddition of 2-naphthol **1a** and phenol **7a** with ethyl vinyl ether (**9a**), and comparison with conventional oxidation methods using a stoichiometric amount of Ag₂O or MnO₂. Self-dimerization or trimerization reactions competed with the desired [4 + 2] cycloaddition under conventional oxidation conditions even in the presence of an excess amount of dienophile.

The relative stereochemistry of **10ia** was confirmed by single-crystal X-ray diffraction analysis, and others were assigned by analogy. The efficiency of this method was further demonstrated by the oxidation of α -tocopherol on a gram scale, using 0.5 mol% **6d** in the presence of potassium carbonate²⁰ to afford **11ha** in 86% yield,

albeit with a prolonged reaction time. Consistent with previous reports, a regioselective oxidation proceeded at the 5-methyl group²⁵ to give a diastereomeric mixture of product²⁶. Notably, as in that of the oxidative coupling of **1a** or **7a** with **9a** (Fig. 2e), the use of Ag₂O as an oxidant gave inferior results for the oxidative cycloaddition

Table 1 | Oxidative tandem [4 + 2] cycloaddition of naphthols (1) and phenols (7) with dienophiles (9)

^aResults of comparison experiments with Ag₂O (1.1 equiv.). Generally, a dimer or trimer was observed as a main product along with several unidentified side products. ^b**9c** (2 equiv.) was used. ^cCommercially available isomeric mixture of **9d** (Z/E = 2:1) was used. ^d**9h** (5 equiv.) was used. ^eK₂CO₃ (1 equiv.) was used as an additive to regenerate the catalytic active species from inert species under low catalyst loading²⁰. A longer reaction time (6 d) was required in the absence of K₂CO₃. ^fCHP (2 equiv.) was used. cPent, cyclopentyl.

of **1a** with other nucleophiles **9b–h** (Table 1; for details, see Supplementary Table 4). Especially, unreacted **1a** was almost recovered when thioether **9e** was used as a coupling partner. However, similar to that of conventional oxidative generation methods¹, our hypiodite catalysis is currently limited to electron-rich phenols. Phenols without electron-donating substituents and/or extended

conjugation could not be oxidized under these mild conditions, or a complex mixture was obtained under harsh conditions possibly due to the instability of the corresponding *o*-QMs under these conditions (see Supplementary Fig. 2 for unsuccessful phenols examined). Nevertheless, phenols **10e–g** bearing synthetically useful halogen substituents along with electron-donating alkoxy groups

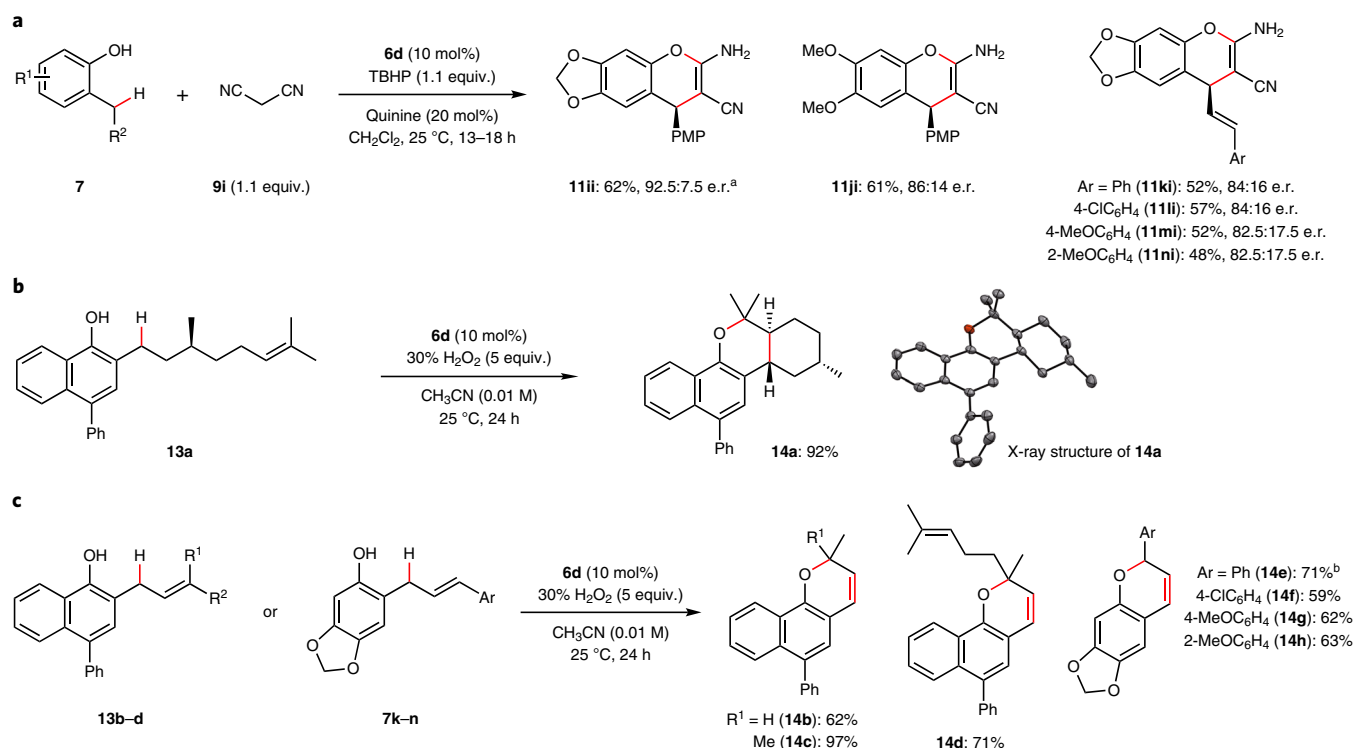


Fig. 3 | Inter- and intramolecular tandem oxidative [4 + 2] cycloaddition. **a**, Merging chiral organobase catalysis and hypiodite catalysis. A tandem process that included hypiodite-catalysed oxidative generation of *o*-QM from phenols and quinine-catalysed enantioselective [4 + 2] cycloaddition of *o*-QMs with malononitrile^{11,31} afforded 2-amino-3-cyano-4*H*-chromenes with good enantioselectivity. **b**, Oxidative intramolecular [4 + 2] cycloaddition. Tetracyclic **14a** could be obtained from the oxidation of 1-naphthol **13a** tethered to a chiral aliphatic alkenyl group in 92% yield as a single diastereomer, which was confirmed by single-crystal X-ray diffraction analysis. Hydrogen atoms are omitted for clarity. Grey, carbon; red, oxygen. **c**, Chemoselective oxidative oxa-6 π -electrocyclization of 1-naphthols (**13b–d**) and phenols (**7k–n**). Corresponding chromenes **14b–h** could be obtained in good to high yields. ^aQuinine (10 mol%) was used. ^bComparison experiment with Ag₂O (1.1 equiv.) gave **14e** in 47% yield along with several unidentified side products.

could be oxidized smoothly to give the corresponding cycloadducts **11** in excellent yields (Table 1).

Recently, there has been rapid progress in the development of enantioselective reactions that harness *o*-QM intermediates^{21,27,28}. Merging it with chiral organobase catalysis, our oxidative generation method could be successively applied to enantioselective oxidative cycloaddition. We succeeded in the asymmetric synthesis of 2-amino-3-cyano-4*H*-chromenes **11ii–ni**, core structures²⁹ or key precursors³⁰ of various bioactive molecules via a tandem process that included hypiodite-catalysed oxidative generation of *o*-QM from phenols **7i–n** and quinine-catalysed^{11,31} enantioselective [4 + 2] cycloaddition with malononitrile (**9i**) (Fig. 3a).

Less electron-rich dienophiles such as styrene or simple aliphatic alkenes, which were used for oxidative [4 + 2] cycloaddition reactions using Ag₂O under harsh reaction conditions (100 °C)¹², could not be used as an intermolecular coupling partner for the present oxidative cycloaddition under mild conditions. However, with the use of a tethered aliphatic alkenyl group possessing a chiral citronellyl group at the 2-position, intramolecular oxidative [4 + 2] cycloaddition of 1-naphthol **13a** proceeded smoothly to give tetracyclic **14a** in 92% yield as a single diastereomer (Fig. 3b). Notably, the use of an excess amount of 30 wt% hydrogen peroxide (5 equiv.) under diluted conditions was crucial to induce the intramolecular reaction of *o*-QM preferentially. The relative stereochemistry of **14a**, which was confirmed by single-crystal X-ray diffraction analysis, suggests that the intramolecular [4 + 2] cycloaddition might proceed via an *exo*-oriented transition state with *E*-configured *o*-QM¹. Similarly, oxa-6 π -electrocyclization of 1-naphthols **13b–d** and phenols **7k–n** with tethered allyl groups at the 2-position proceeded smoothly to

give the corresponding chromenes **14b–h** in good to high yields (Fig. 3c). Notably, oxidative electrocyclization of 2-geranyl-1-naphthol **14d** proceeded preferentially with an internal alkene.

Next, we were interested in oxidative conjugate addition reactions (Fig. 4). Oxidative conjugate addition through *o*-QMs has rarely been reported and is limited to specialized substrates^{1,22,32}. The hypiodite-catalysed oxidative C–N coupling of 2-naphthol **1a** or 1-naphthol **1e** with succinimide (5 equiv.) using hydrogen peroxide in the presence of potassium carbonate afforded the corresponding 1,4-adduct **15a** or **15b** in good to high yields (Fig. 4a). Notably, oxidative dimerization of **1** proceeded preferentially in the absence of base additives, which might activate the nucleophile in these cases. By contrast, oxidative coupling of 2,4,6-trimethylphenol (**7o**) with an equimolar amount of succinimide or phthalimide (at the gram scale) proceeded smoothly even in the absence of base additives, presumably due to the formation of stable *p*-QM instead of *o*-QM, which is prone to dimerization, to give the corresponding 1,6-adducts **15c** and **15d** in high yields (Fig. 4b). As expected, *p*-QMs were formed more readily than *o*-QMs under oxidative conditions because *p*-QMs are more stable than *o*-QMs¹. Oxidative conjugate 1,6-addition of **7o** proceeded efficiently under mild conditions with various nucleophiles such as azoles (**15e–g**), methanol (**15h**), acetic acid (**15i**), *N*-Boc-L-serine (**15j**) and azide (**15k**) (Fig. 4b,c). By sharp contrast, the use of Ag₂O as a stoichiometric oxidant gave much lower yields (**15a** and **15m**) or complex reaction mixtures (**15d** and **15h**). Additionally, almost-unreacted phenol **7o** was recovered for **15f**, **15g** and **15j** under these conventional oxidation conditions. Chemoselective and divergent oxidative azidation of **7o** was achieved in the presence of an equimolar or excess

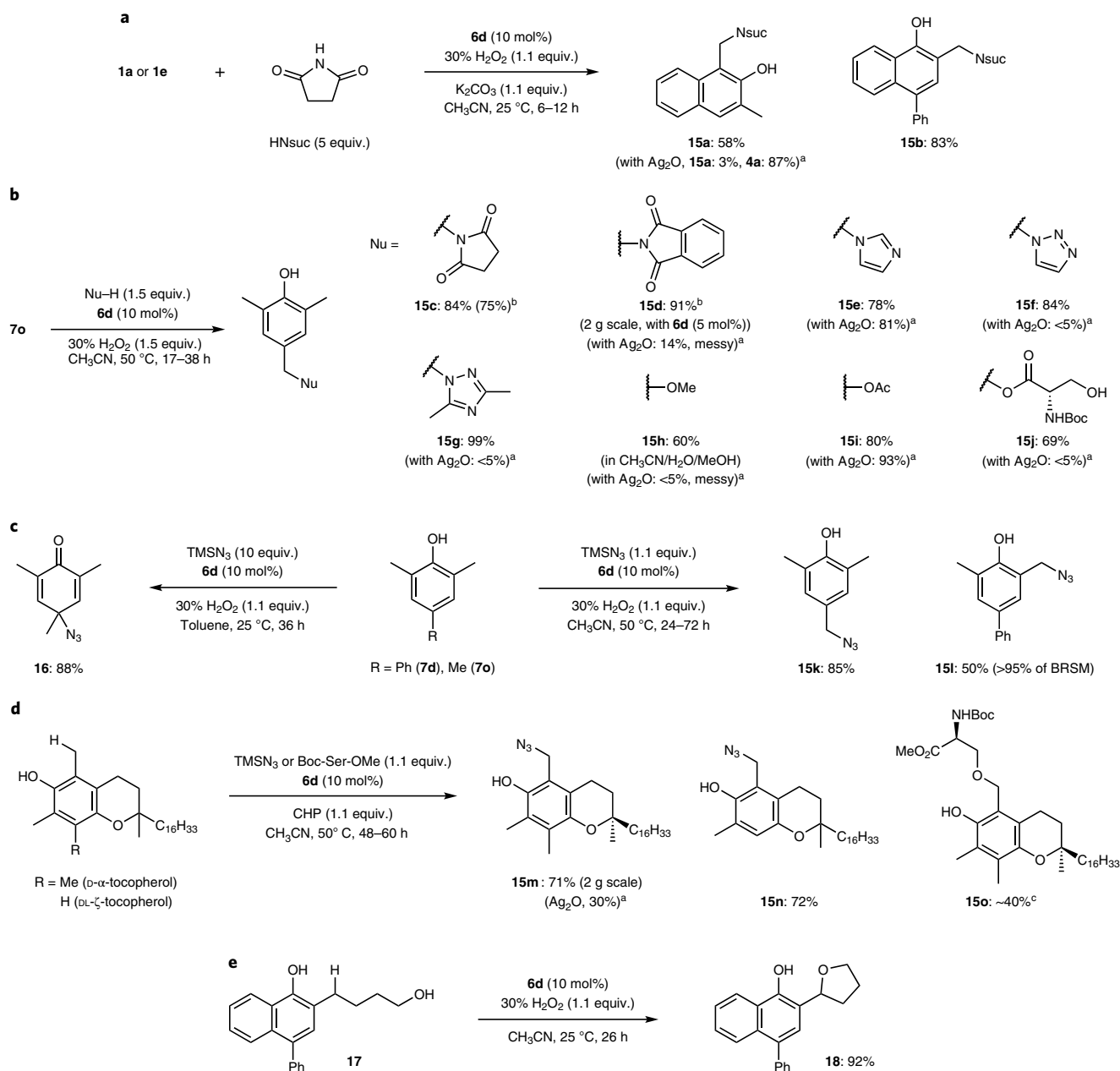


Fig. 4 | Tandem oxidative conjugate addition. **a**, Oxidative 1,4-conjugate addition of naphthols **1** with succinimide (HNsuc). Because of the high reactivity of naphthols and their *o*-QM derivatives towards oxidation and subsequent self-dimerization, respectively, base additives were required to enhance the desired conjugate coupling reactions, presumably via the activation of nucleophiles. **b**, Oxidative 1,6-conjugate addition of phenol **7o** with various nucleophiles, which were found to be difficult to use (except for acetic acid and benzimidazole) in conventional oxidative methods using Ag₂O. In addition, because *p*-QMs are stable and unsuitable to self-dimerization, base additives were not required. **c**, Chemoselective and divergent conjugate (right) or dearomatized (left) azidation reactions enabled by simply changing the reaction conditions. BRSM, based on recovered starting material. **d**, Oxidative conjugate addition of tocopherols. Tocopheryl azides **15m** and **15n** could be easily synthesized from the regio- and chemoselective oxidative azidation of α- and ζ-tocopherols, respectively. Although oxidative conjugation of α-tocopherol with *N*-Boc-L-serine methyl ester (Boc-Ser-OMe) could be confirmed by NMR and LC-MS analysis (see 'Oxidative conjugation of D-α-tocopherol with *N*-Boc-L-serine methyl ester' in the Supplementary Information), we failed to isolate the product **15o** due to its rapid decomposition during the purification process. **e**, Chemoselective intramolecular oxa-conjugate cyclization of **17**. ^aComparison experiments with Ag₂O (1.1 equiv.) at 50 °C. ^bNuH (1.1 equiv.) and 30% H₂O₂ (1.1 equiv.) were used. ^cBoc-Ser-OMe (3.0 equiv.), 70 °C, 24 h. Yield was determined by ¹H NMR analysis of crude.

amount of trimethylsilyl azide (TMSN₃) to afford 1,6-adduct **15k** or dearomatized product **16**³³, respectively, in high yields (Fig. 4c). Furthermore, tocopheryl azides **15m** (at the 2 g scale) and **15n** could be easily synthesized from the regio-²⁵ and chemoselective oxidative azidation of α- and ζ-tocopherols, respectively (Fig. 4d). Notably, **15m** has been used in the glyco- or peptido-conjugation

of interest in several biological studies^{34–36}; however, multistep synthetic sequences have been required³⁴. To the best of our knowledge, these oxidative C–N coupling reactions have not been reported and provide a new entry to the synthesis of benzylic amine derivatives. Additionally, oxidative conjugation of α-tocopherol with *N*-Boc-L-serine methyl ester could be confirmed by nuclear magnetic

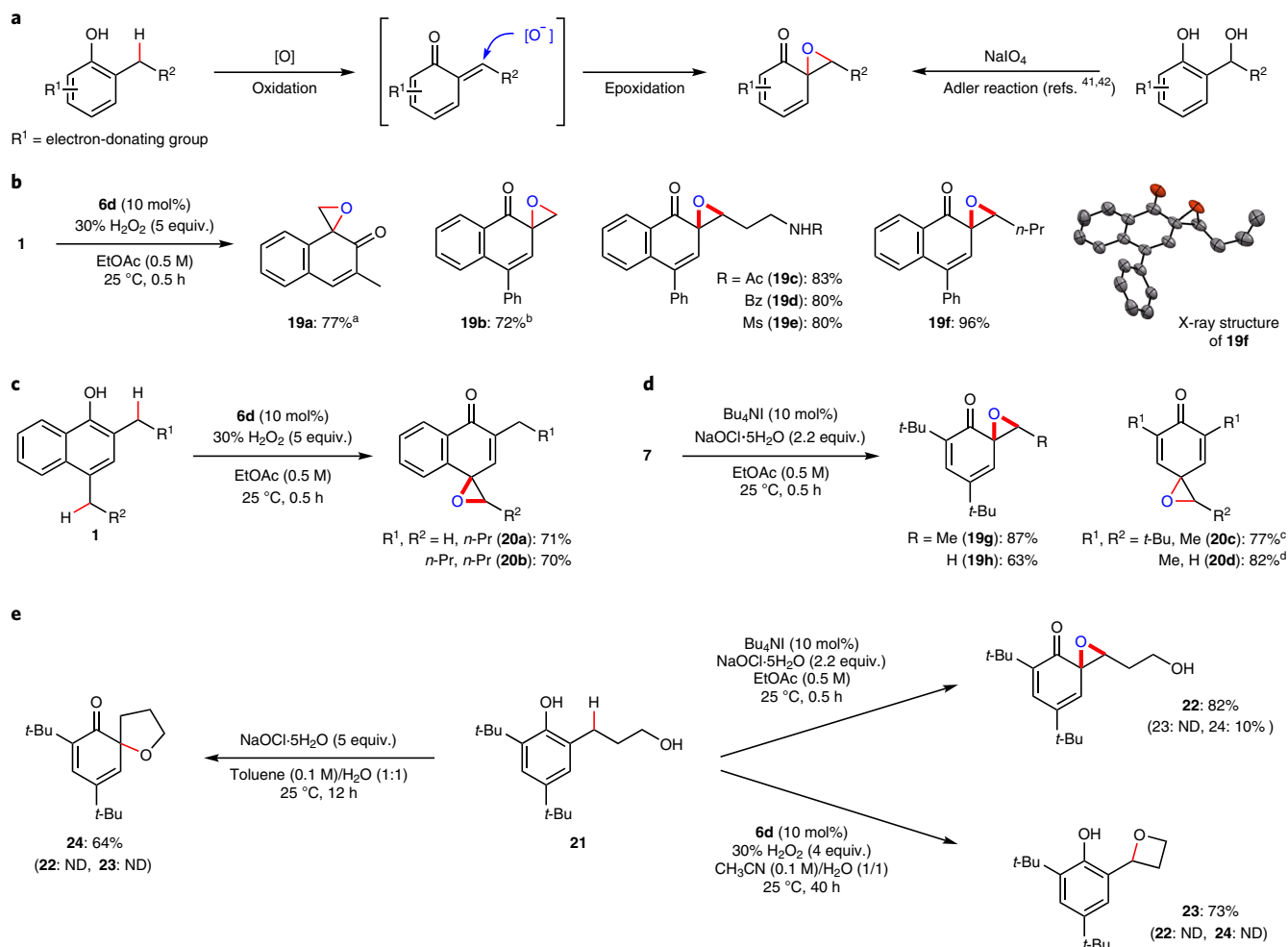


Fig. 5 | Oxidative spiroepoxidation of phenols. **a**, A catalytic, direct oxidative spiroepoxidation of phenols (this work) and the Adler reaction, which is the oxidative dearomative spiroepoxidation of salicylic alcohols using sodium periodate as a stoichiometric oxidant. Oxidative spiroepoxidation would proceed via a conjugate addition of a nucleophilic oxidant to QMs generated in situ. **b**, Chemoselective spiroepoxidation of 1- and 2-naphthols **1** via corresponding *o*-QMs using hydrogen peroxide. Oxidation of 1-naphthols bearing secondary alkyl groups at the benzylic positions gave the corresponding *trans*-epoxides exclusively, which was confirmed by single-crystal X-ray diffraction analysis. Hydrogen atoms are omitted for clarity. Grey, carbon; red, oxygen. **c**, A *para*-selective spiroepoxidation of 2,4-dialkyl-1-naphthols via the corresponding *p*-QMs. Because *p*-QMs are more stable than *o*-QMs, *p*-QMs were formed more readily than *o*-QMs. **d**, Chemoselective spiroepoxidation of phenols **7** using sodium hypochlorite pentahydrate as an oxidant. The use of hydrogen peroxide as an oxidant in acetonitrile or ethyl acetate gave **19g** in less than 10% yield. For details, see Supplementary Table 6. **e**, Oxidant-dependent chemoselective and divergent intermolecular spiroepoxidation (right top), intramolecular cycloetherification (right bottom) and dearomative spiroetherification (left) of phenol **21**. For details, see Supplementary Table 7. ^aReaction time was 1.5 h. ^b60 wt% H_2O_2 was used. ^c1.9 g scale. ^d $NaOCl \cdot 5H_2O$ (3 equiv.) was used in mixed EtOAc/ H_2O (1:1, v/v.). ND, not determined.

resonance (NMR) and liquid chromatography–mass spectrometry (LC-MS) analysis; however, the isolation of the product **15o** failed due to rapid decomposition presumably via the formation of the corresponding unstable *o*-QM during the purification process. On the other hand, the intramolecular oxidative 1,4-addition of 1-naphthol **17** with a tethered aliphatic hydroxyl group at the 2-position proceeded smoothly to give tetrahydrofuran **18** in excellent yield (Fig. 4e).

The highly electrophilic nature of QMs prompted us to develop a new oxidative transformation, that is, the oxidative spiroepoxidation of 2- or 4-alkylarenols. We envisioned that spiroepoxidation would proceed via a conjugate addition of a nucleophilic oxidant to QMs (Fig. 5a)^{37,38}. To the best of our knowledge, there has been no report of a similar tandem transformation that uses QMs generated oxidatively from *ortho*- or *para*-alkylarenols for spiroepoxidation reactions. While our manuscript was being prepared, Johnson reported an elegant approach to enantioselective

dearomative spiroepoxidation via QM intermediates that are generated in situ from 2- or 4-hydroxybenzyl alcohol derivatives under basic conditions^{39,40}. Adler first reported the oxidative dearomative spiroepoxidation of salicylic alcohols using stoichiometric quantities of sodium periodate as an oxidant⁴¹. Later, the Adler reaction was used as a highly useful tool for the synthesis of various natural products and biologically active compounds⁴². Our tandem spiroepoxidation protocol would complement the Adler reaction. We investigated the reaction parameters for the oxidative spiroepoxidation of **1a** (see Supplementary Table 5 for details), and found that dimerization could be suppressed with the use of an excess amount of hydrogen peroxide (5 equiv.) under concentrated conditions, and spiroepoxide **19a** was obtained in 77% yield (Fig. 5b). Notably, the use of Ag_2O or MnO_2 as a stoichiometric oxidant in the presence of hydrogen peroxide gave only **4a** along with several side products, and no trace of spiroepoxide **19a** was observed.

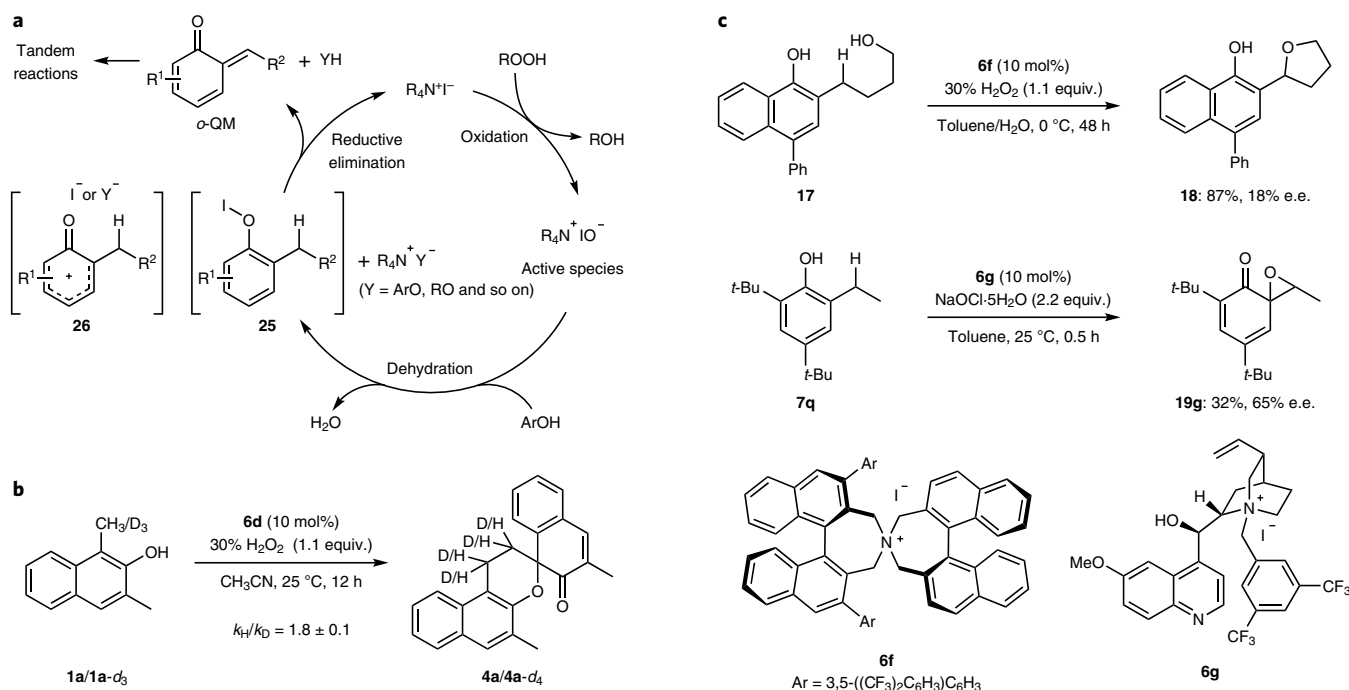


Fig. 6 | Reaction mechanism and enantioselective reactions. **a**, Proposed reaction mechanism based on the experimental results and previous works^{19,20,33}. Kinetics studies suggested that reductive elimination might be the rate-determining step in the catalytic cycle. For details, see Supplementary Figs. 4–6. **b**, The secondary kinetic isotope effect was observed to be 1.8 for the oxidative dimerization of **1a/1a-d₃**, which suggests that β -deprotonation might proceed after dissociation to phenoxenium **26**. **c**, Preliminary results of the enantioselective oxidative coupling reactions. Intramolecular oxa-conjugate cyclization of **17** and spiroepoxidation of **7q** gave the corresponding products **18** and **19g** with moderate enantioselectivity. The absolute configuration of each of these products was not determined.

The oxidation of various 1-naphthols **1** with hydrogen peroxide under the optimized conditions gave the corresponding spiroepoxides **19** in high yield (Fig. 5b). Notably, *trans*-epoxides **19c–f** were obtained selectively from the oxidation of the corresponding 1-naphthols bearing secondary alkyl groups at the benzylic positions. The relative stereochemistry of **19f** was confirmed by single-crystal X-ray diffraction analysis, and others were assigned by analogy. Moreover, *para*-selective oxidation of 2,4-dialkyl-1-naphthols **1** afforded the corresponding spiroepoxides **20a** and **20b** derived from the corresponding *p*-QMs, as observed in *para*-selective oxidative conjugate addition described above (Fig. 5c). The relative stereochemistry of these *trans*-epoxides, which were the sole diastereomer isolated, was confirmed by a NOe analysis.

However, the oxidation of phenols **7** using hydrogen peroxide was sluggish, and the desired *ortho*- or *para*-spiroepoxides **19** or **20** were obtained in low yield. Unproductive decomposition of hydrogen peroxide by hypoiodite catalysis⁴³ might proceed under these conditions due to the lower reactivity of phenols towards oxidative dearomatization compared with that of naphthols^{44,45}. Additionally, due to the high tendency towards peroxidative dearomatization¹⁹, alkyl hydroperoxides (TBHP and CHP) could not be used efficiently as oxidants for the spiroepoxidation reactions. The chemoselective spiroepoxidation of phenols **7** proceeded smoothly to give spiroepoxides **19** or **20** in high yields with the use of sodium hypochlorite pentahydrate⁴⁶ as an oxidant (Fig. 5d; see Supplementary Tables 6 and 7 for details). Tetrabutylammonium iodide was found to be an optimal catalyst because the ammonium cation of catalyst **6d** decomposed under these strong oxidative conditions. Moreover, a gram-scale oxidation gave *para*-epoxide **20c** in 77% yield. Notably, the use of a conventional aqueous solution of sodium hypochlorite gave a complex reaction mixture, and spiroepoxide was isolated in low yield.

The efficiency of the hypoiodite catalysis was further demonstrated by the divergent chemoselective oxidation of phenol **21** with a tethered aliphatic hydroxyl group at the 2-position (Fig. 5e). An intermolecular oxidative epoxidation proceeded preferentially with the use of sodium hypochlorite pentahydrate as an oxidant to afford spiroepoxide **22** in 82% yield. Although hydrogen peroxide could not be used efficiently for the spiroepoxidation of phenols, the intramolecular oxidative 1,4-addition of **21** proceeded to give oxetane **23** in 73% yield when hydrogen peroxide was used in aqueous acetonitrile under diluted conditions (see Supplementary Table 7 for details). Moreover, sodium hypochlorite is a strong oxidant that can promote the oxidation of phenols in the absence of an iodide catalyst; however, dearomative intramolecular cyclization⁴⁷ proceeded via a Friedel–Crafts-type *ortho*-chlorination⁴⁸ followed by intramolecular cyclization to give spiroether **24** in 64% yield. Thus, the oxidation of a catalytic amount of iodide with sodium hypochlorite to an iodine-based active species would proceed preferentially under these conditions to lead to the unprecedented chemoselective oxidation of phenols.

To gain insight into the catalytic mechanism for the oxidative generation of *o*-QMs, we performed various control experiments (see Supplementary Table 9 for details) and concluded that the hypoiodite species may be a catalytically active species^{15,20}. Furthermore, the addition of radical scavengers such as *N*-tert-butyl- α -phenylnitrone (PBN), 1,1-diphenylethylene and 2,2,6,6-tetramethyl-1-piperidinyloxy (TEMPO) did not influence the yield in the oxidative dimerization of **1a**, suggesting that a free-radical pathway might be unlikely. Based on these experimental results and previous works^{19,20,33}, a proposed mechanism is depicted in Fig. 6a. Ammonium hypoiodite could be generated in situ as an active species from the oxidation of ammonium iodide with an oxidant. A reversible dehydration reaction of arenol with the hypoiodite

species might afford an aryl hypoiodite intermediate **25**, which might give *o*-QM via the reductive elimination of ammonium iodide directly or after dissociation⁴⁹ to the phenoxenium cation **26**. The β -deprotonation process might be helped by the base species ($R_4N^+Y^-$, $Y = ArO$, RO , and so on) generated in situ catalytically.

To gain further insight into the mechanism of the generation of *o*-QMs, we performed kinetic studies using the oxidative dimerization of **1a** as a model reaction (see Supplementary Figs. 4–6). The reaction rate was found to have a first-order dependence on the concentration of catalyst **6d** and a zero-order dependence on both substrate **1a** and hydrogen peroxide. These results suggest that reductive elimination might be the rate-determining step in the catalytic cycle (Fig. 6a). Finally, the secondary kinetic isotope effect (KIE)⁵⁰ for the oxidative dimerization of **1a** and **1a-d₃** in separate vessels based on the initial reaction rates was observed to be 1.8 (Fig. 6b), which suggests that β -deprotonation might proceed after dissociation to phenoxenium **26** (Fig. 6a). Therefore, electrostatic or hydrogen-bonding interactions⁵¹ between the leaving iodide and the ammonium cation centre or acidic α -hydrogen atoms of the highly reactive catalyst **6d**, respectively, might enhance the reactivity of the dissociative reductive elimination step.

The highly reactive *o*-QMs generated in situ would then react rapidly with a suitable nucleophile to give the corresponding coupling products. The ammonium cation of the catalyst might not bind strongly enough to the pro-chiral *o*-QMs to induce stereoselectivity during this process. Indeed, no asymmetric induction was encountered with the use of chiral ammonium iodides for the oxidative cycloaddition or electrocyclization reactions. On the other hand, some attractive interactions would be expected with the anionic nucleophiles⁵¹, which enable the asymmetric induction during the conjugate addition of *o*-QMs. Intramolecular oxa-conjugate cyclization of **17** and spiroepoxidation of **7q** in the presence of chiral ammonium iodides **6f**²⁰ or **6g**³⁹, respectively, gave the corresponding products **18** and **19g** with moderate enantioselectivity (Fig. 6c). These preliminary results revealed the feasibility of the use of this ammonium hypoiodite catalysis for the enantioselective oxidative coupling reaction through *o*-QM intermediates.

In summary, we have developed a transition-metal-free catalytic oxidative generation of *o*-QMs using hypoiodite catalysis through the oxidation of *ortho*-alkylarenes and applied *o*-QMs as transient reactive intermediates to tandem reactions. Inexpensive tetrabutyl- or tetramethylammonium iodides or sodium iodide could be used as a catalyst. Moreover, to induce higher reactivity, a new structurally compact quinuclidine-derived quaternary ammonium iodide catalyst has also been designed. A mechanistic investigation suggests that the rate-determining step of the present catalysis might be the dissociative reductive elimination of iodide from the aryl hypoiodite intermediate. This method for the chemoselective generation of *o*-QMs is superior to previous methods with respect to not only environmental issues but also the wider scope, especially with respect to coupling partners, and could be applied to various oxidative tandem reactions such as inter- or intramolecular [4+2] cycloaddition (including self-dimerization or trimerization and enantioselective cycloaddition), oxa-6 π -electrocyclization, inter- or intramolecular conjugate addition with nitrogen or oxygen nucleophiles and spiroepoxidation. Strikingly, several chemoselective divergent oxidative couplings could be achieved by simply changing the reaction conditions.

Online content

Any Nature Research reporting summaries, source data, extended data, supplementary information, acknowledgements, peer review information; details of author contributions and competing interests; and statements of data and code availability are available at <https://doi.org/10.1038/s41557-020-0433-4>.

Received: 13 March 2019; Accepted: 29 January 2020;
Published online: 23 March 2020

References

- Van de Water, R. W. & Pettus, T. R. R. *o*-Quinone methides: intermediates underdeveloped and underutilized in organic synthesis. *Tetrahedron* **58**, 5367–5405 (2002).
- Rokita, S. E. (ed.) *Quinone Methides* (John Wiley and Sons, 2009).
- Ferreira, S. B., da Silva, Fd., Pinto, A. C., Gonzaga, D. T. & Ferreira, V. F. Syntheses of chromenes and chromanes via *o*-quinone methide intermediates. *J. Heterocycl. Chem.* **46**, 1080–1097 (2009).
- Willis, N. J. & Bray, C. D. *ortho*-Quinone methides in natural product synthesis. *Chem. Eur. J.* **18**, 9160–9173 (2012).
- Jaworski, A. A. & Scheidt, K. A. Emerging roles of in situ generated quinone methides in metal-free catalysis. *J. Org. Chem.* **81**, 10145–10153 (2016).
- Peter, M. G. Chemical modifications of biopolymers by quinones and quinone methides. *Angew. Chem. Int. Ed.* **28**, 555–570 (1989).
- Moore, H. W. Bioactivation as a model for drug design bioreductive alkylation. *Science* **197**, 527–532 (1977).
- Moore, R. F. & Waters, W. A. Some products formed from phenolic inhibitors during the autoxidation of cumene. *J. Chem. Soc.* **1954**, 243–246 (1954).
- Liao, D., Li, H. & Lei, X. Efficient generation of *ortho*-quinone methide: application to the biomimetic syntheses of (\pm)-schefflone and tocopherol trimers. *Org. Lett.* **14**, 18–21 (2012).
- Osipov, D. V., Osyanin, V. A. & Klimochkin, Y. N. Easy access to (\pm)-schefflone and espintanol. *Synlett* 917–919 (2012).
- Wu, B., Gao, X., Yan, Z., Chen, M.-W. & Zhou, Y.-G. C-H oxidation/Michael addition/cyclization cascade for enantioselective synthesis of functionalized 2-amino-4H-chromenes. *Org. Lett.* **17**, 6134–6137 (2015).
- Wong, Y. F., Wang, Z., Hong, W.-X. & Sun, J. A one-pot oxidation/cycloaddition cascade synthesis of 2,4-diaryl chromans via *ortho*-quinone methides. *Tetrahedron* **72**, 2748–2751 (2016).
- Gebauer, K., Reuf, F., Spanka, M. & Schneider, C. Relay catalysis: manganese(III) phosphate catalyzed asymmetric addition of β -dicarbonyls to *ortho*-quinone methides generated by catalytic aerobic oxidation. *Org. Lett.* **19**, 4588–4591 (2017).
- Oguma, T. et al. Iron-catalyzed asymmetric inter- and intramolecular aerobic oxidative dearomatizing spirocyclization of 2-naphthols. *Asian J. Org. Chem.* <https://doi.org/10.1002/ajoc.201900602> (2020).
- Uyanik, M. & Ishihara, K. Catalysis with in situ-generated (hypo)iodite ions for oxidative coupling reactions. *ChemCatChem* **4**, 177–185 (2012).
- Finkbeiner, P. & Nachtsheim, B. J. Iodine in modern oxidation catalysis. *Synthesis* **45**, 979–999 (2013).
- Chen, R., Chen, J., Zhang, J. & Wan, X. Combination of tetrabutylammonium iodide (TBAI) with *tert*-butyl hydroperoxide (TBHP): an efficient transition-metal-free system to construct various chemical bonds. *Chem. Rec.* **18**, 1292–1305 (2018).
- Becker, P., Duhamel, T., Stein, C. J., Reiher, M. & Muñiz, K. Cooperative light-activated iodine and photoredox catalysis for the amination of C_{sp^3} -H bonds. *Angew. Chem. Int. Ed.* **56**, 8004–8008 (2017).
- Uyanik, M., Nishioka, K. & Ishihara, K. Ammonium hypoiodite-catalyzed peroxidative dearomatization of phenols. *Heterocycles* **95**, 1132–1147 (2017).
- Uyanik, M., Hayashi, H. & Ishihara, K. High-turnover hypoiodite catalysis for asymmetric synthesis of tocopherols. *Science* **345**, 291–294 (2014).
- Yang, B. & Gao, S. Recent advances in the application of Diels–Alder reactions involving *o*-quinodimethanes, aza-*o*-quinone methides and *o*-quinone methides in natural product total synthesis. *Chem. Soc. Rev.* **47**, 7926–7953 (2018).
- Patel, A., Netscher, T. & Rosenau, T. Stabilization of *ortho*-quinone methides by a bis(sulfonium ylide) derived from 2,5-dihydroxy-[1,4]benzoquinone. *Tetrahedron Lett.* **49**, 2442–2445 (2008).
- Chen, P. K. C., Wong, Y. F., Yang, D. & Pettus, T. R. R. Nucleophilic imines and electrophilic *o*-quinone methides, a three-component assembly of assorted 3,4-dihydro-2H-1,3-benzoxazines. *Org. Lett.* **21**, 7746–7749 (2019).
- Arduini, A., Bosi, A., Pochini, A. & Ungaro, R. *o*-Quinone methides 2. Stereoselectivity in cycloaddition reactions of *o*-quinone methides with vinyl ethers. *Tetrahedron* **41**, 3095–3103 (1985).
- Dean, F. M. & Orabi, M. O. A. Spirans. Part 15. The effect of ring size upon the regioselective oxidative coupling of heterocyclic phenols. *J. Chem. Soc. Perkin Trans. 1* **1982**, 2617–2624 (1982).
- Schröder, H. & Netscher, T. Determination of the absolute stereochemistry of vitamin E derived oxa-spiro compounds by NMR spectroscopy. *Magn. Reson. Chem.* **39**, 701–708 (2001).
- Pathak, T. P. & Sigman, M. S. Applications of *ortho*-quinone methide intermediates in catalysis and asymmetric synthesis. *J. Org. Chem.* **76**, 9210–9215 (2011).
- Caruana, L., Fochi, M. & Bernardi, L. The emergence of quinone methides in asymmetric organocatalysis. *Molecules* **20**, 11733–11764 (2015).

29. Shestopalov, A. M. et al. Polyalkoxy substituted 4*H*-chromenes: synthesis by domino reaction and anticancer activity. *ACS Comb. Sci.* **14**, 484–490 (2012).
30. Maalej, E. et al. Synthesis, biological assessment, and molecular modeling of racemic 7-aryl-9,10,11,12-tetrahydro-7*H*-benzo[7,8]chromeno[2,3-*b*]quinolin-8-amines as potential drugs for the treatment of Alzheimer's disease. *Eur. J. Med. Chem.* **54**, 750–763 (2012).
31. Adili, A., Tao, Z.-L., Chen, D.-F. & Han, Z.-Y. Quinine-catalyzed highly enantioselective cycloannulation of *o*-quinone methides with malononitrile. *Org. Biomol. Chem.* **13**, 2247–2250 (2015).
32. Angle, S. R., Rainier, J. D. & Woytowicz, C. Synthesis and chemistry of quinone methide models for the anthracycline antitumor antibiotics. *J. Org. Chem.* **62**, 5884–5892 (1997).
33. Uyanik, M., Nishioka, K. & Ishihara, K. Ammonium hypiodite-catalyzed oxidative dearomatization azidation of arenols. *Chem. Lett.* **48**, 353–356 (2019).
34. Adewöhler, C., Rosenau, T., Kloser, E., Mereiter, K. & Netscher, T. Synthesis of 5a- α -tocopheryl azide and its reaction to 1-(5a- α -tocopheryl)-1,2,3-triazols by [2+3]-cycloaddition. *Eur. J. Org. Chem.* **2006**, 2081–2086 (2006).
35. Lahmann, M. & Thiem, J. Transformations of chromanol and tocopherol and synthesis of ascorbate conjugates. *Tetrahedron* **67**, 1654–1664 (2011).
36. Browne, E. C., Langford, S. C. & Abbott, B. M. Synthesis and effects of conjugated tocopherol analogues on peptide nucleic acid hybridization. *Org. Biomol. Chem.* **11**, 6744–6750 (2013).
37. Lattanzi, A. Advances in asymmetric epoxidation of α,β -unsaturated carbonyl compounds: the organocatalytic approach. *Curr. Org. Synth.* **5**, 117–133 (2008).
38. Lifchits, O. et al. The cinchona primary amine-catalyzed asymmetric epoxidation and hydroperoxidation of α,β -unsaturated carbonyl compounds with hydrogen peroxide. *J. Am. Chem. Soc.* **135**, 6677–6693 (2013).
39. McLaughlin, M. F., Massolo, E., Liu, S. & Johnson, J. S. Enantioselective phenolic α -oxidation using H₂O₂ via an unusual double dearomatization mechanism. *J. Am. Chem. Soc.* **141**, 2645–2651 (2019).
40. McLaughlin, M. F., Massolo, E., Cope, T. A. & Johnson, J. S. Phenolic oxidation using H₂O₂ via in situ generated *para*-quinone methides for the preparation of *para*-spiroepoxydienones. *Org. Lett.* **21**, 6504–6507 (2019).
41. Adler, E., Brasen, S. & Miyake, H. Periodate oxidation of phenols. *Acta Chem. Scand.* **25**, 2055–2069 (1971).
42. Singh, V. Spiroepoxycyclohexa-2,4-dienones in organic synthesis. *Acc. Chem. Res.* **32**, 324–334 (1999).
43. Uyanik, M. et al. High-performance hypiodite/hydrogen peroxide catalytic system for the oxylactonization of aliphatic γ -oxocarboxylic acids. *Chem. Lett.* **44**, 387–389 (2015).
44. Uyanik, M. & Ishihara, K. in *Asymmetric Dearomatization Reactions* (ed. You, S.-L.) 129–151 (Wiley-VCH, 2016).
45. Bordwell, F. G. & Cheng, J. Substituent effects on the stabilities of phenoxyl radicals and the acidities of phenoxyl radical cations. *J. Am. Chem. Soc.* **113**, 1736–1743 (1991).
46. Kirihaara, M. et al. Sodium hypochlorite pentahydrate crystals (NaOCl·5H₂O): a convenient and environmentally benign oxidant for organic synthesis. *Org. Process Res. Dev.* **21**, 1925–1937 (2017).
47. Uyanik, M., Sasakura, N., Kuwahata, M., Ejima, Y. & Ishihara, K. Practical oxidative dearomatization of phenols with sodium hypochlorite pentahydrate. *Chem. Lett.* **44**, 381–383 (2015).
48. Uyanik, M., Sahara, N. & Ishihara, K. Regioselective oxidative chlorination of arenols using NaCl and oxone. *Eur. J. Org. Chem.* **2019**, 27–31 (2019).
49. Swenton, J. S., Carpenter, K., Cheng, Y., Kerns, M. L. & Morrow, G. W. Intramolecular anodic carbon-carbon bond-forming reactions of oxidized phenol intermediates leading to spirodienones. Structural effects on reactivity and evidence for a phenoxonium ion intermediate. *J. Org. Chem.* **58**, 3308–3316 (1993).
50. Gómez-Gallego, M. & Sierra, M. A. Kinetic isotope effects in the study of organometallic reaction mechanisms. *Chem. Rev.* **111**, 4857–4863 (2011).
51. Shirakawa, S. et al. Tetraalkylammonium salts as hydrogen-bonding catalysts. *Angew. Chem. Int. Ed.* **54**, 15767–15770 (2015).

Publisher's note Springer Nature remains neutral with regard to jurisdictional claims in published maps and institutional affiliations.

© The Author(s), under exclusive licence to Springer Nature Limited 2020

Data availability

All data generated and analysed during this study are included in this Article and its Supplementary Information. Crystallographic data for the structures reported in this Article have been deposited at the Cambridge Crystallographic Data Centre, under deposition numbers CCDC 1893878 (**8a**), 1893879 (**10ia**), 1893880 (**14a**) and 1893881 (**19f**). Copies of the data can be obtained free of charge via www.ccdc.cam.ac.uk/data_request/cif.

Acknowledgements

Financial support for this project was partially provided by JSPS.KAKENHI (15H05755 (to K.I.), 15H05810 (to K.I.), 15H05484 (to M.U.), 18H01973 (to M.U.)), Inoue Research Award for Young Scientists (to M.U.), and the Program for Leading Graduate Schools: IGER Program in Green Natural Sciences (MEXT). We thank T. Yasui, K. Ohori, N. Sahara and O. Katade for their assistance during the initial investigations. We thank K. Nishimura for electrospray ionization-mass spectrometry analysis. We are grateful to the Kaneka Corporation and Mitsubishi Gas Chemical Co. for providing NaOCl·5H₂O and 60 wt% H₂O₂, respectively.

Author contributions

M.U. and K.I. developed the concept and conceived the experiments. K.N. and R.K. performed the experiments. K.N., R.K. and M.U. analysed the data. M.U. prepared the manuscript with assistance from K.I.

Competing interests

The authors declare no competing interests.

Additional information

Supplementary information is available for this paper at <https://doi.org/10.1038/s41557-020-0433-4>.

Correspondence and requests for materials should be addressed to K.I.

Reprints and permissions information is available at www.nature.com/reprints.